

Installation of d3-methyl group to drugs by continuous-flow solid-phase synthesis

Received: 1 May 2025

Accepted: 22 October 2025

Published online: 28 November 2025

 Check for updates

Wei Ou^{1,2,6}, Hao Hou^{1,6}, Ying Tao¹, Qiyuan Wang³, Taoran Chen¹, Jie Wang¹, Wei Liu¹, Qingzhu Xu³, Lei Yu³, Bin Liu^{1,2,4,5} & Chenliang Su^{1,2,✉}

The d3-methyl group, which combines the “magic methyl effect” and the deuterium effect, is highly sought after by medicinal chemists, resulting in the development of various d3-methyl reagents derived from low-cost, readily available CD₃OD. However, a universally applicable, cost-effective, easily accessible and handleable, highly active, and recyclable d3-methyl reagent remains elusive. Herein, we design a thianthrene-based organic polymer (TT-OP) that shows the ability of capturing and releasing the d3-methyl reagent. This polymer demonstrates excellent loading capacity, scalability, and stability. Utilizing this developed heterogeneous d3-methyl reagent (TT-OP-CD₃), we achieve selective d3-methylation of over 35 biologically active molecules d3-at oxygen, nitrogen, sulfur, and carbon sites—transformations that are very challenging to be realized by other methods. Finally, we establish an automated platform for high-throughput, scalable d3-methylation of pharmaceutical molecules by integrating solid-phase synthesis with continuous-flow, demonstrating its sustainability and practicality for drug synthesis.

The methyl group is one of the most fundamental and simplest structural units in synthetic and medicinal chemistry, playing a crucial role in numerous biological processes, including DNA replication, protein modification, and various metabolic pathways^{1–3}. Introducing a methyl group into drug molecules can effectively improve their solubility and target selectivity, prolong their half-life *in vivo*, and reduce the IC₅₀ value. For instance, incorporating methyl functional groups into the ant cardiovascular drug simvastatin doubled its half-life, while the efficacy of the antibody OX1R increased by 480 times compared to its precursor⁴. The colloquial term “magic methyl effect” is often used to describe these unique advantages in the medicinal chemistry community^{5–8}. Deuterium-labeled compounds are widely employed as analytical tools for investigating reaction mechanisms and elucidating metabolic pathways^{9–12}. In addition, due to the deuterium isotope effect, where C–D bonds exhibit higher dissociation energies than C–H

bonds, substituting hydrogen atoms in drugs with deuterium can significantly enhance their absorption, distribution, metabolism, and excretion properties^{13–15}.

Consequently, the d3-methyl group, which combines the “magic methyl effect” and the deuterium effect, is highly valued by medicinal and organic chemists^{16–18}. Notably, among the five currently approved deuterated drugs, three contain deuterated methyl groups, and several d3-methyl-containing molecules are under clinical investigation (Fig. 1). To meet this demand, various d3-methyl reagents have been developed, including CD₃I, d6-DMSO, CD₃CO₂D, CD₃OD, and derivatives based on CD₃OD^{19–33}. Although CD₃OD stands out as the most cost-effective and readily accessible d3-methyl reagent, its direct application is constrained by the requirement for a specialized catalytic system and its relatively low reactivity, limiting its general applicability^{24–29}. Therefore, there is an urgent need to develop a universally applicable, cost-effective, readily

¹International Collaborative Laboratory of 2D Materials for Optoelectronics Science and Technology of Ministry of Education, Institute of Microscale Optoelectronics, Shenzhen University, Shenzhen, P. R. China. ²Shenzhen Key Laboratory of 2D Metamaterials for Information Technology, Shenzhen University, Shenzhen, P. R. China. ³College of Chemistry and Chemical Engineering, Yangzhou University, Yangzhou, China. ⁴Department of Materials Science and Engineering, City University of Hong Kong, Hong Kong, SAR, P. R. China. ⁵Department of Chemistry, Hong Kong Institute of Clean Energy (HKICE) & Center of Super-Diamond and Advanced Films (COSDAF), City University of Hong Kong, Hong Kong, P. R. China. ⁶These authors contributed equally: Wei Ou, Hao Hou. ✉ e-mail: chmsuc@szu.edu.cn

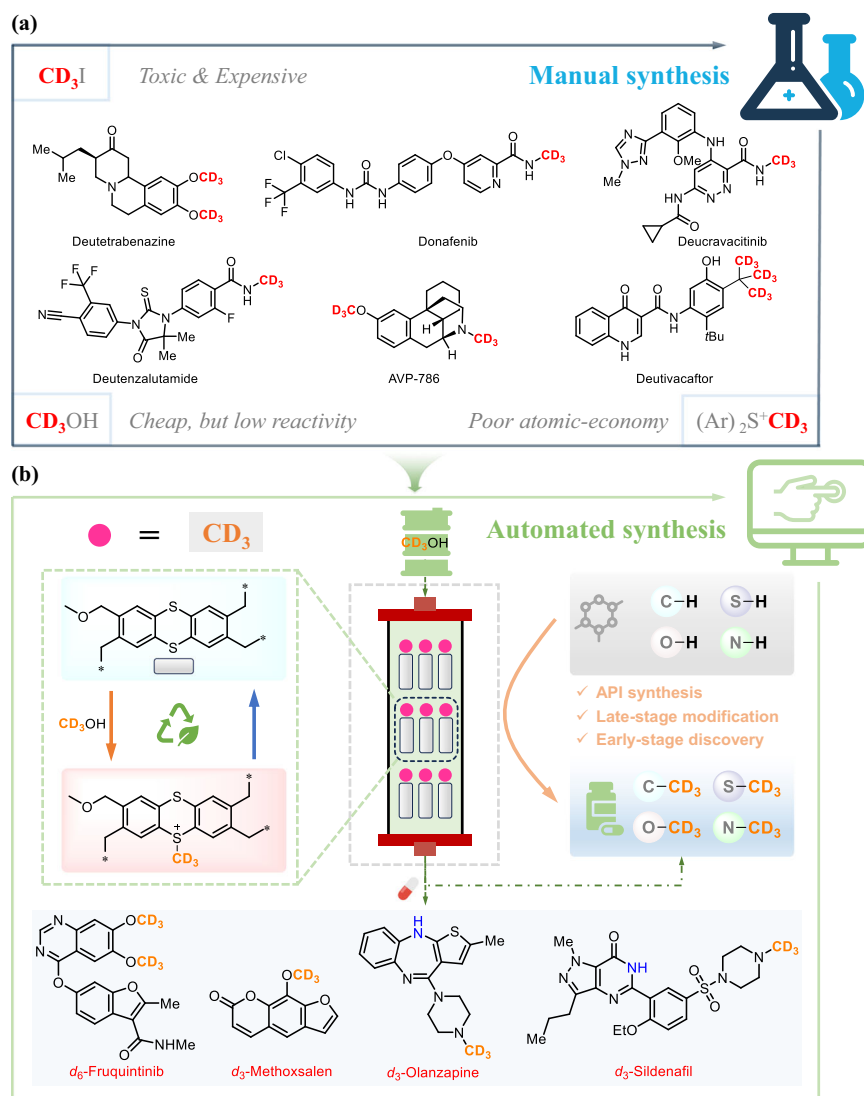


Fig. 1 | Project design. **a** Traditional homogeneous d3-methyl reagents and bioactive molecules containing d3-methyl groups. **b** From manual to automated synthesis of d3-methyl bioactive molecules by SPS-based continuous-flow platform. SPS solid-phase synthesis.

accessible, easily handleable, highly active, and recyclable d3-methyl reagent derived from CD₃OD.

Recently, Wu's group reported an automated platform that integrates solid-phase synthesis (SPS)^{34–38} with a continuous-flow system for the automated synthesis of prexasertib derivatives³⁹. This strategy, combining SPS and continuous-flow processing, unlocks new avenues for automated synthesis. Inspired by this and the biochemistry of S-adenosylmethionine in living organisms^{40,41}, we here develop a thianthrene-based organic polymer (TT-OP) that has the capability to capture and release the d3-methyl derived from CD₃OD. Impressively, TT-OP can be scaled up to hectogram-scale quantities and exhibits excellent immobilization capability for the d₃-methyl group, yielding TT-OP-CD₃ with a maximum loading capacity of approximately 80%. The solid TT-OP-CD₃ demonstrates highly selective and universal capability for d3-methylating bioactive molecules at oxygen, nitrogen, sulfur, and carbon sites, delivering the desired pharmaceutical products and regenerating the TT-OP, which remains super-stable and reusable for over 50 runs. This property of TT-OP enables us to establish a program-controlled, SPS-based continuous-flow automation platform, offering a clean, universal, and high-throughput d3-methylation method for the late-stage modification of a wide range of pharmaceutical molecules, easily accessible via a push-button interface.

Results

Synthesis and characterization of TT-OP and TT-OP-CD₃

Thianthrene (TT)-based polymers (TT-OP) were prepared via an anhydrous FeCl₃-mediated^{42,43} Friedel–Crafts alkylation reaction, utilizing formaldehyde dimethyl acetal (FDA) as a cross-linker under a nitrogen atmosphere (Fig. 2a). Using this polymerization method, TT-OP could be readily synthesized on a hectogram scale (Supplementary Information). As shown in Fig. 2b, c, solid-state cross-polarization/magic angle spinning nuclear magnetic resonance (¹³C CP/MAS NMR) spectroscopy and Fourier transform infrared (FT-IR) spectroscopy measurements confirmed the successful crosslinking of TT-OP by FDA. The signal observed at approximately 40 ppm in the ¹³C CP/MAS NMR spectrum and the weak peak at around 2920 cm⁻¹ in the FT-IR spectrum were attributed to the –CH₂– groups, along with minor remnants of –CH₂OCH₃ in the polymer. UV-visible diffuse reflectance spectroscopy (UV-vis DRS) spectrum reveals that TT is a near-ultraviolet-sensitive material, whereas the absorption edge of TT-OP extends to approximately 800 nm, resulting in its reddish-brown color (Fig. 2d). With TT-OP in hand, we next evaluated its capability to load CD₃ groups using CD₃OTf, which could be generated in situ from CD₃OD and Tf₂O. To confirm successful loading, solid-state ²H magic angle spinning nuclear magnetic resonance (MAS NMR) spectroscopy was

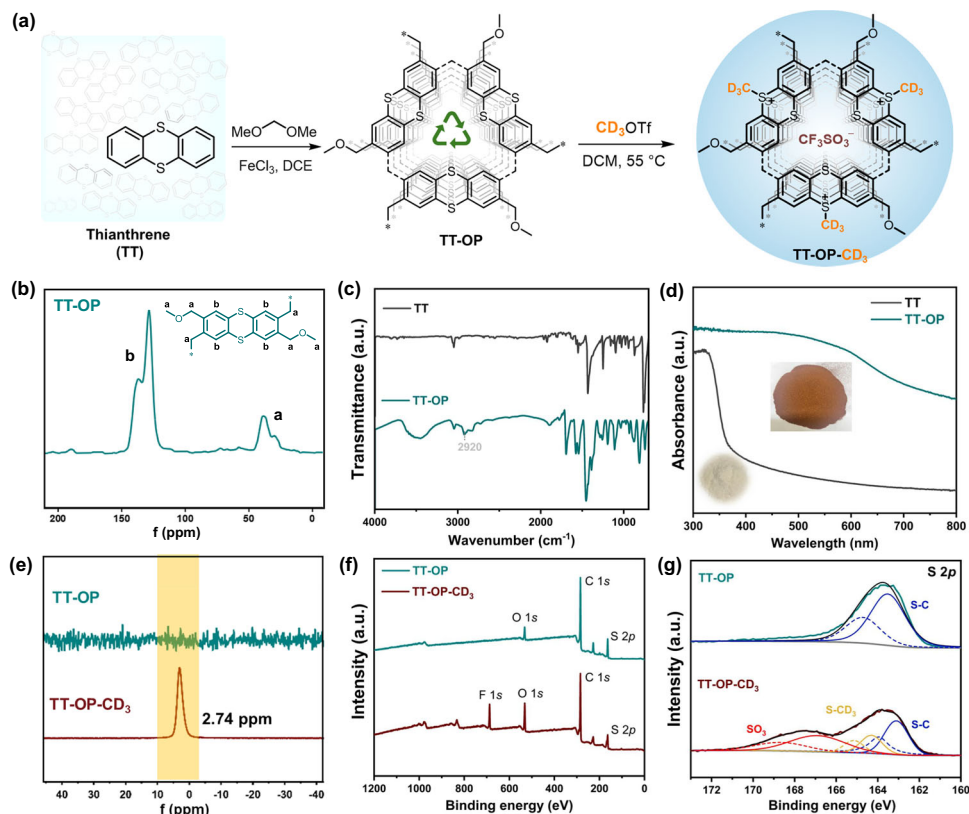


Fig. 2 | Synthesis and characterization of TT-OP and TT-OP-CD₃. **a** Synthetic procedure of TT-OP and TT-OP-CD₃. **b** Solid-state ¹³C CP/MAS NMR spectrum of TT-OP. **c** FT-IR spectra of TT and TT-OP. **d** UV-vis absorption diffuse reflectance spectra of TT and TT-OP. **e** Solid-state ²H MAS NMR of TT-OP and TT-OP-CD₃. **f** XPS survey spectra of TT-OP and TT-OP-CD₃. **g** S 2p XPS spectra of TT-OP and TT-OP-CD₃.

performed. As depicted in Fig. 2e, the spectrum of TT-OP-CD₃ exhibits a distinct peak at 2.74 ppm, corresponding to the CD₃ group. The elemental composition of TT-OP and TT-OP-CD₃, determined by survey XPS, is shown in Fig. 2f. Notably, an additional F 1s peak appears in the TT-OP-CD₃ XPS spectrum, with a binding energy of 689 eV, consistent with the CF₃SO₃⁻ counterion associated with sulfonium⁴⁴. High-resolution XPS analysis of the S 2p signal further elucidates the formation of the S-CD₃ bond (Fig. 2g). The S 2p XPS spectrum of TT-OP shows one spin-orbit split doublet (2p_{3/2} and 2p_{1/2}), characteristic of the S-C (aromatic) bond. While this peak is retained in the TT-OP-CD₃ XPS spectrum, deconvolution of the broadened S 2p signal reveals a new S species (sulfonium) at a higher binding energy, consistent with the binding of CD₃ groups to sulfur sites, which likely involves electron donation from sulfur to the CD₃ groups. In addition, there appears a new peak with significantly higher binding energy in the TT-OP-CD₃ XPS spectrum, corresponding to the CF₃SO₃⁻ group⁴⁵. To quantify the amount of S-bound CD₃ groups, d3-methylation of N-methylaniline using TT-OP-CD₃ was conducted, demonstrating that more than 0.12 mmol of CD₃ groups were loaded per 100 mg of TT-OP-CD₃ polymer (see Supplementary Information for details).

Substrate scope

With the TT-OP-CD₃ in hands, the selectivity of TT-OP-CD₃ and three other commercially available d3-methyl reagents (CD₃I, CD₃OTf, and (CD₃)₂SO₄) were investigated. When a substrate with three nucleophilic sites was treated with these reagents, the results showed that TT-OP-CD₃ exhibited the best selectivity and the highest yield (see Supplementary Information for details). After identification of the good selectivity and reactivity of TT-OP-CD₃, various pharmaceuticals, natural products, and their derivatives containing multiple potential reactive sites were evaluated under optimized reaction conditions

(Fig. 3). Beginning with d3-methylation of carboxylic acid-based pharmaceutical molecules, we were pleased to find that, irrespective of whether complex primary, secondary, or tertiary carboxylic acids were used, the d3-methylation products (**2a–2h**) were obtained in yields ranging from 83% to 97%. The heterogeneous nature of the d3-methylation reagent enabled high-purity products to be achieved through simple filtration and extraction. Notably, the d3-methyl esterification reaction exhibited excellent selectivity and functional group tolerance, effectively accommodating substrates containing nucleophilic amino, secondary amide, and phenolic groups, as well as sensitive functionalities such as aldehydes, ketones, alkenes, and heterocyclic units. To demonstrate the practicality, late-stage functionalization of pharmaceuticals, including bezafibrate, d-biotin, niflumic acid, carprofen, repaglinide, frusemide, and mycophenolic acid, was performed, delivering the corresponding d3-methyl esterification products (**2i–2o**) with N-H or O-H bonds preserved in the desired yields. This strategy also provides a reliable and rapid method for deuterium-switching of methyl ester drugs. Commercially available drugs such as clopidogrel and bifendate were readily converted to their corresponding deuterated variants (**2p** and **2q**) through a simple two-step process (alkali-promoted hydrolysis followed by d3-methylation with TT-OP-CD₃), achieving total yields of 79%–85%.

Next, this strategy was applied to phenols. Selective d3-methylation of phenolic hydroxyl groups was achieved to afford products (**2r–2v**) in high yields. Methoxsalen, commonly used in combination with UVA light therapy (PUVA therapy) to treat psoriasis—a chronic skin condition characterized by scaly, red patches—represents a relevant example. Deuterium substitution at the methyl ether has the potential to improve its first-pass effect and photostability. Notably, methoxsalen was effectively converted into d3-methoxsalen (**2t**) with 78% total yield. The ortho-dimethyl ether (veratrole) motif frequently

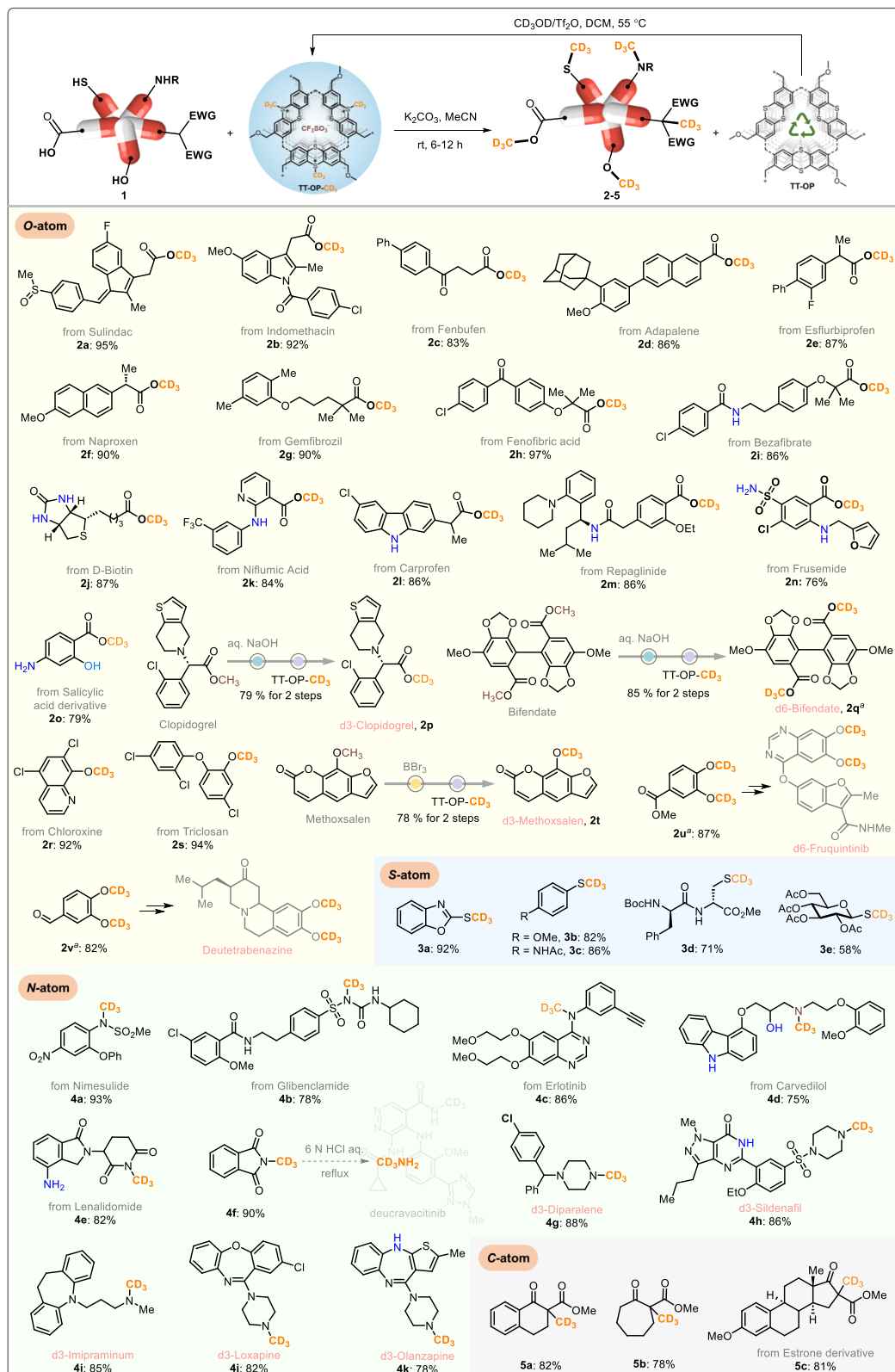


Fig. 3 | Substrate scope of the d3-methylation using TT-OP-CD₃. Reaction conditions: **1** (0.5 mmol), TT-OP-CD₃ (500 mg), K₂CO₃ (1.0 mmol), and MeCN (5 mL), rt, 12 h. Isolated yields. ^aTT-OP-CD₃ (1000 mg), K₂CO₃ (2.0 mmol) were used.

serves as a metabolic site in pharmaceutical molecules⁴⁶. Using this heterogeneous d3-methylation approach, the key deuterated building blocks **2u** and **2v** for deutetabenazine (SD-809, the first approved deuterated drug) and deuterated fruquintinib were smoothly obtained in 87% and 82% yields, respectively. Then, we explored S-alkylation,

which plays a significant role in chemical biology. For example, S-alkylation modifications of cysteine-containing peptides have been extensively employed in activity-based protein profiling^{47–49}. Consequently, we examined S-atom d3-methylation using TT-OP-CD₃. Under the standard reaction conditions, both aryl thiophenols and

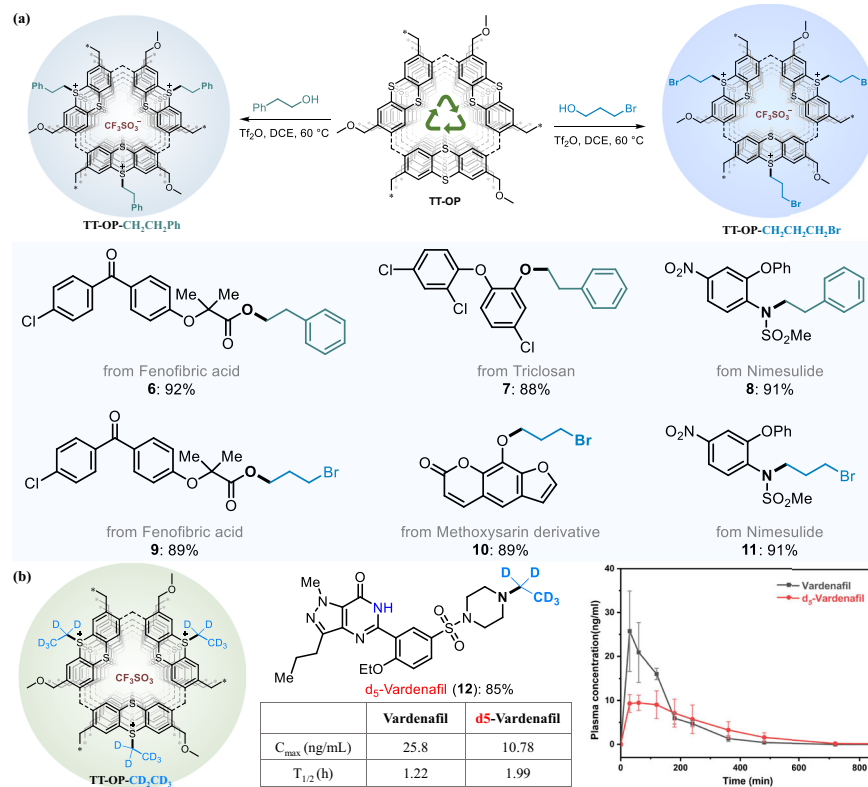


Fig. 4 | Extension and application. **a** Preparation and reaction of other heterogeneous alkylating reagents. **b** The application of TT-OP-CD₂CD₃ in d5-vardenafil and its pharmacokinetic study. Error bars represent the standard deviation of five independent rats' data.

biologically active cysteine-containing peptides or 1-thioglycosides were effectively and selectively S-d3-methylated to afford the corresponding products (**3a**–**3e**) in yields ranging from 82% to 92%.

The late-stage functionalization of sulfonamides and secondary amines was also investigated. Nimesulide, a non-steroidal anti-inflammatory and anti-rheumatic drug, was successfully d3-methylated to yield **4a** in 93% yield. To evaluate the selectivity toward N–H units, glibenclamide, which bears three types of N–H bonds, was employed. As expected, selective d3-methylation occurred at the sulfonamide N–H unit (**4b**) due to its lower pK_a value. Erlotinib, a small molecule tyrosine kinase inhibitor, reacted smoothly with TT-OP-CD₃ to produce the nitrogen d3-methylated compound **4c**, while preserving the terminal alkyne group. When carvedilol, which contains an O–H bond and two N–H bonds, was used as a substrate, selective d3-methylation at the carbazole N–H bond was observed, delivering product **4d** in 75% yield. Similarly, lenalidomide, which contains both an active aryl-amino group and an imide group, was treated with TT-OP-CD₃ under standard conditions, affording **4e** in 82% yield with the active amino group intact. The **4f** serves as a crucial precursor in the synthesis of d3-methylamine, which is the direct deuterium source for sorafenib. Our synthetic strategy enables the rapid and efficient one-step synthesis of compound **4f** in high yield, streamlining the production process. Next, various N-CD₃ drugs, including d3-diparalene (**4g**), d3-sildenafil (**4h**), d3-imipramine (**4i**), d3-loxapine (**4j**), and d3-olanzapine (**4k**), were smoothly obtained in yields ranging from 78% to 88%. Furthermore, the heterogeneous TT-OP-CD₃ reagent also proved effective for d3-methylation of active methylene groups using five-, six-, and seven-membered cyclic β-ketoesters, producing the corresponding products (**5a**–**5c**) in good yields. In summary, the heterogeneous deuterated d3-methyl reagent demonstrated an ability for selective and clean d3-methylation at oxygen, nitrogen, sulfur, and carbon sites with unique selectivity and excellent functional group tolerance, overcoming challenges typically faced by other methylation reagents.

The ability to load other alkylating reagents onto TT-OP for sequential alkylation was further investigated (Fig. 4). Phenethyl-containing and bromopropyl-containing thianthrenium salts (designated TT-OP-CH₂CH₂Ph and TT-OP-CH₂CH₂CH₂Br, respectively) were successfully prepared and applied to esterification, etherification, and sulfonamide alkylation, yielding the corresponding alkylated products (**6**–**11**). Notably, although TT-OP-CH₂CH₂CH₂Br possesses two electrophilic sites, alkylation occurred exclusively at the sulfonium site. Vardenafil, one of the most widely used drugs for the treatment of male erectile dysfunction⁵⁰, is primarily metabolized in the liver via cytochrome P450 (CYP) 3A4, with its main metabolite being the N-desethylated form of the piperazine structure⁵¹. To study the metabolic effects, d5-vardenafil (**12**) was specifically prepared, and its plasma concentrations were measured following oral administration in rats. The results demonstrated that d5-vardenafil (**12**) exhibited a lower C_{max} (maximum plasma concentration) and a longer t_{1/2} (biological half-life) compared to vardenafil, confirming the improved pharmacokinetic profile of d5-vardenafil.

SPS-based continuous-flow platform

The stability of TT-OP is of significant importance for multirun experiments and the smart SPS-based continuous-flow d3-methylation platform. Impressively, our results indicated the exceptional stability of TT-OP, which could be recovered and reused more than 50 times without any loss of its loading ability or reactivity (Fig. 5a). Encouraged by this remarkable stability, we designed and developed a program-controlled SPS-based continuous-flow d3-methylation platform (Fig. 5b). This platform consists of four syringe pumps, switching valves, a tower reactor with an interlayer, a programmable heating bath system, and a software controller. The four syringe pumps correspond to four channel systems controlled by the software program: line 1 is the loading channel with the DCE solution of CD₃OTf; lines 2 and 4 are the washing channels with MeCN and DCE solution, respectively; line 3 is the d3-methylation

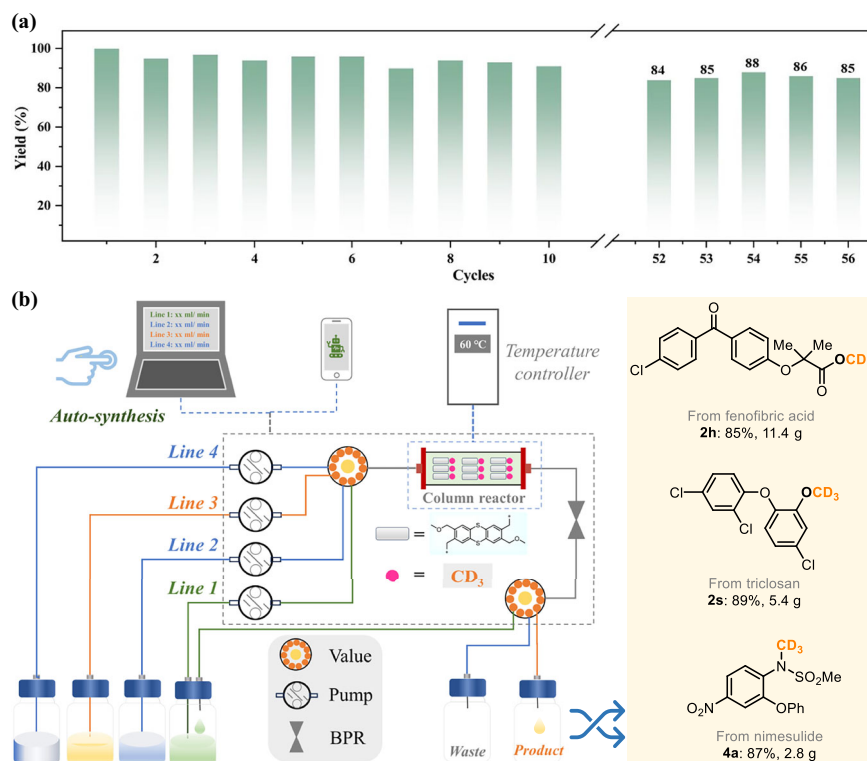


Fig. 5 | Development of SPS-based continuous-flow platform. a More than 50 reuse cycles of TT-OP. **b** Platform for d3-methylated bioactive molecule production. SPS solid-phase synthesis, BPR Back Pressure Regulator.

channel with MeCN solution of substrate. To validate the concept, the d3-methylation reactions of fenofibrate, nimesulide, and triclosan at gram to decagram scales were conducted on this platform. Taking fenofibric acid as an example, the DCE solution of CD_3OTf (20 mmol) on line 1 was initially pumped through the tower reactor containing 40 g of TT-OP at a flow rate of 10 mL/min, at 55 °C for 8 h. Subsequently, the MeCN solution on line 2 was pumped to remove residual CD_3OTf /DCE (10 mL/min, 20 min, 25 °C). Following this, fenofibrate (10 mmol, 3.19 g) and K_2CO_3 (20 mmol, 2.8 g) dissolved in a MeCN/H₂O mixture (250/50 mL) on line 3 were pumped through the tower reactor at a rate of 0.8 mL/min. The residence time within the reactor was maintained at 3 h, after which the mixture flowed into a product bottle, yielding d3-methyl fenofibrate (2.85 g) in 85% yield. Finally, the DCE solution on line 4 was pumped at a rate of 10 mL/min for 20 min to restore the initial state of the reactor. Notably, all four steps could be executed automatically with a single click of the “start” button via a computer or mobile phone control program. By replenishing the starting materials in each container and leveraging the programmed reaction sequence, the system could sustain multiple reaction cycles. Ultimately, we obtained 11.4 g of compound **2h**, 5.4 g of compound **2s**, and 2.8 g of compound **4a**, with average yields exceeding 85%.

Discussion

In summary, we have successfully designed a TT-OP with excellent capability for immobilizing d3-methyl groups, yielding TT-OP-CD₃. The solid TT-OP-CD₃ demonstrates highly selective and efficient d3-methylation of carboxylic acids, phenols, amines, amides, thiols, and β -ketoesters, delivering a variety of significant deuterated pharmaceuticals and simultaneously releasing the support. Notably, TT-OP exhibits exceptional stability that can be reused for more than 50 runs without any loss of loading capacity and reactivity. These features enable us to establish an automated platform for high-throughput d3-methylation of pharmaceutical molecules by integrating SPS with continuous-flow. This program-controlled platform offers several

remarkable and unique advantages: 1. Very simple and automatic operation: The process requires only the addition of starting materials, followed by a single click of the start button to produce the desired products. 2. Powerful capability for late-stage modification: The platform can selectively incorporate d3-methyl groups at oxygen, nitrogen, sulfur, and carbon sites of pharmaceutical molecules and natural products. In addition, it accommodates other alkylation reactions (e.g., ethyl, phenethyl, and bromoalkyl) by simply switching the reagents in the reservoir and pressing the start button. 3. Straightforward scale-up mode: Continuous addition of starting materials enables flow synthesis for large-scale production. In conclusion, the automated d3-methylation platform, characterized by its long-term stability, low-cost support and deuterium source, and ease of operation and purification, holds great promise for smart, efficient, and practical applications in pharmaceutical synthesis.

Methods

General procedure for d3-methylation of carboxylic acid, phenol, amine, thiol, and active methylene

To the Schlenk tube was added substrate (0.5 mmol, 1.0 equiv), TT-OP-CD₃ (500 mg), K_2CO_3 (1.0 mmol, 138.2 mg, 2.0 equiv), and MeCN (5 mL). The reaction was stirring at room temperature for 12 h. After the reaction, the recyclable TT-OP was simply centrifuged at 10000 rpm (10610 g) for 10 min and was washed with dichloromethane (5 mL) three times, dried under vacuum, and directly reused for the next reaction cycle without any further purification. The organic layers were combined, dried over anhydrous Na_2SO_4 , and concentrated in vacuo. The residue was purified by chromatography on silica gel or without further purification to afford desired product.

Data availability

Data supporting the findings of this manuscript are reported within the Article and its Supplementary Information and are also available from the corresponding author upon request.

References

1. Roundtree, I., Evans, A., Pan, M. E. & He, T. C. Dynamic RNA modifications in gene expression regulation. *Cell* **169**, 1187–1200 (2017).
2. Harcourt, E. M., Kietrys, A. M. & Kool, E. T. Chemical and structural effects of base modifications in messenger RNA. *Nature* **541**, 339–346 (2017).
3. Barreiro, E. J., Kummerle, A. E. & Fraga, C. A. M. The methylation effect in medicinal chemistry. *Chem. Rev.* **111**, 5215–5246 (2011).
4. Cox, C. D. et al. Conformational analysis of *N*, *N*-disubstituted 1,4-diazepane orexin receptor antagonists and implications for receptor binding. *Bioorg. Med. Chem. Lett.* **19**, 2997–3001 (2009).
5. Sun, S. & Fu, J. Methyl-containing pharmaceuticals: methylation in drug design. *Bioorg. Med. Chem. Lett.* **28**, 3283–3289 (2018).
6. Schönherr, H. & Cernak, T. Profound methyl effects in drug discovery and a call for new C–H methylation reactions. *Angew. Chem. Int. Ed.* **52**, 12256–12267 (2013).
7. Aynedtinova, D. et al. Installing the “magic methyl” – C–H methylation in synthesis. *Chem. Soc. Rev.* **50**, 5517–5563 (2021).
8. Huang, J., Chen, Z. & Wu, J. Recent progress in methyl-radical-mediated methylation or demethylation reactions. *ACS Catal.* **11**, 10713–10732 (2021).
9. Ou, W., Qiu, C. & Su, C. Photo- and electro-catalytic deuteration of feedstock chemicals and pharmaceuticals: a review. *Chin. J. Catal.* **43**, 956–970 (2022).
10. Ou, W. et al. Room-temperature palladium-catalyzed deuteration of carbon oxygen bonds towards deuterated pharmaceuticals. *Angew. Chem. Int. Ed.* **60**, 6357–6361 (2021).
11. Simmons, E. M. & Hartwig, J. F. On the interpretation of deuterium kinetic isotope effects in C–H bond functionalizations by transition-metal complexes. *Angew. Chem. Int. Ed.* **51**, 3066–3072 (2012).
12. Atzrodt, J., Derdau, V., Kerr, W. J. & Reid, M. Deuterium- and tritium-labelled compounds: applications in the life sciences. *Angew. Chem. Int. Ed.* **57**, 1758–1784 (2018).
13. Martino, R. M. C. D., Maxwell, B. D. & Pirali, T. Deuterium in drug discovery: progress, opportunities and challenges. *Nat. Rev. Drug Discov.* **22**, 562–584 (2023).
14. Derdau, V., Atzrodt, J., Zimmermann, J., Kroll, C. & Brückner, F. Hydrogen–deuterium exchange reactions of aromatic compounds and heterocycles by NaBD₄-activated rhodium, platinum and palladium catalysts. *Chem. Eur. J.* **15**, 10397–10404 (2009).
15. Chen, J., Zhu, Y.-Y., Huang, L., Zhang, S.-S. & Gu, S.-X. Application of deuterium in research and development of drugs. *Eur. J. Med. Chem.* **287**, 117371 (2025).
16. Schmidt, C. First deuterated drug approved. *Nat. Biotechnol.* **35**, 493–494 (2017).
17. Goyal, V. et al. Recent advances in the catalytic *N*-methylation and *N*-trideuteromethylation reactions using methanol and deuterated methanol. *Coord. Chem. Rev.* **474**, 214827 (2023).
18. Pipal, R. W. et al. Metallaphotoredox aryl and alkyl radiomethylation for PET ligand discovery. *Nature* **589**, 542–547 (2021).
19. Davenport, E., Negru, D. E., Badman, G., Lindsay, D. M. & Kerr, W. J. Robust and general late-stage methylation of Aryl chlorides: application to isotopic labeling of drug-like scaffolds. *ACS Catal.* **13**, 11541–11547 (2023).
20. Caporaso, R. et al. Radical trideuteromethylation with deuterated dimethyl sulfoxide in the synthesis of heterocycles and labelled building blocks. *Chem. Commun.* **52**, 12486 (2016).
21. Shen, Z. et al. Trideuteromethylation enabled by a sulfoxonium metathesis reaction. *Org. Lett.* **21**, 448–452 (2019).
22. Zhu, Q. & Nocera, D. G. Photocatalytic hydromethylation and hydroalkylation of olefins enabled by titanium dioxide mediated decarboxylation. *J. Am. Chem. Soc.* **142**, 17913–17918 (2020).
23. Qi, X. et al. Photoinduced hydrodifluoromethylation and hydro-methylation of alkenes enabled by ligand-to-iron charge transfer mediated decarboxylation. *ACS Catal.* **14**, 1300–1310 (2014).
24. Wang, L., Neumann, H. & Beller, M. Palladium-catalyzed methylation of nitroarenes with methanol. *Angew. Chem. Int. Ed.* **131**, 5417–5421 (2019).
25. Liu, P. et al. From hydrogen autotransfer process to deuterium autotransfer process: the *N*-trideuteromethylation of amines with deuterated methanol to trideuteromethylated amines catalyzed by a Cp⁺Ir complex bearing a flexible bridging and functional ligand. *J. Catal.* **410**, 333–338 (2022).
26. Zhang, Z. et al. Semiconductor photocatalysis to engineering deuterated *N*-alkyl pharmaceuticals enabled by synergistic activation of water and alkanols. *Nat. Commun.* **11**, 4722 (2020).
27. Wu, H. et al. Heterogeneous photocatalytic methanol oxidation coupled with oxygen reduction toward pyrimidines synthesis. *Sci. Bull.* **69**, 2496–2500 (2024).
28. Wang, L.-M. et al. Photocatalytic *N*-methylation of amines over Pd/TiO₂ for the functionalization of heterocycles and pharmaceutical intermediates. *ACS Sustain. Chem. Eng.* **6**, 15419–15424 (2018).
29. Wang, L.-M. et al. *N*-alkylation of functionalized amines with alcohols using a copper–gold mixed photocatalytic system. *Sci. Rep.* **8**, 6931 (2018).
30. Wang, M., Zhao, Y., Zhao, Y. & Shi, Z. Bioinspired design of a robust *d*3-methylating agent. *Sci. Adv.* **6**, eaba0946 (2020).
31. Chen, J. et al. Sulfonium-based precise alkyl transposition reactions. *Sci. Adv.* **9**, eadi1370 (2023).
32. Ban, K. et al. Sulfonium salt reagents for the introduction of deuterated alkyl groups in drug discovery. *Angew. Chem. Int. Ed.* **62**, e202311058 (2023).
33. Qin, L.-Z. et al. The development and application of a novel tri-deuterium methylation reagent. *Cell Rep. Phys. Sci.* **5**, 101843 (2024).
34. Merrifield, B. Solid phase synthesis. *Science* **232**, 341–347 (1986).
35. Guillier, F., Orain, D. & Bradley, M. Linkers and cleavage strategies in solid-phase organic synthesis and combinatorial chemistry. *Chem. Rev.* **100**, 2091–2158 (2000).
36. Nandy, J. P. et al. Advances in solution- and solid-phase synthesis toward the generation of natural product-like libraries. *Chem. Rev.* **109**, 1999–2060 (2009).
37. Plante, O. J., Palmacci, E. R. & Seeberger, P. H. Automated solid-phase synthesis of oligosaccharides. *Science* **291**, 1523–1527 (2001).
38. Mijalis, A. J. et al. A fully automated flow-based approach for accelerated peptide synthesis. *Nat. Chem. Biol.* **13**, 464–466 (2017).
39. Liu, C. et al. Automated synthesis of prexasertib and derivatives enabled by continuous-flow solid-phase synthesis. *Nat. Chem.* **13**, 451–457 (2021).
40. Broderick, J. B., Duffus, B. R., Duschene, K. S. & Shepard, E. M. Radical S-adenosylmethionine enzymes. *Chem. Rev.* **114**, 4229–4317 (2014).
41. Vey, J. L. & Drennan, C. L. Structural insights into radical generation by the radical SAM superfamily. *Chem. Rev.* **111**, 2487–2506 (2011).
42. Zhang, G. et al. Stable, carrier separation tailorabile conjugated microporous polymers as a platform for highly efficient photocatalytic H₂ evolution. *Appl. Catal. B: Environ.* **245**, 114–121 (2019).
43. Ou, W., Zhang, G., Wu, J. & Su, C. Photocatalytic cascade radical cyclization approach to bioactive indoline-alkaloids over donor–acceptor type conjugated microporous polymer. *ACS Catal.* **9**, 5178–5183 (2019).
44. Peter, J., Moinuddin, M. G., Ghosh, S., Sharma, S. K. & Gonsalves, K. E. Organotin in nonchemically amplified polymeric hybrid resist imparts better resolution with sensitivity for next-generation lithography. *ACS Appl. Polym. Mater.* **2**, 1790–1799 (2020).
45. Wang, Z. et al. Sulfonium-functionalized polystyrene-based non-chemically amplified resists enabling sub-13 nm nanolithography. *ACS Appl. Mater. Interfaces* **15**, 2289–2300 (2023).
46. Kumar, A. S., Ghosh, S., Soundararajan, R. & Mehta, G. N. Efficient syntheses of (±)-cherylline and latifine dimethyl ether. *Synth. Commun.* **40**, 1588–1594 (2010).

47. Lv, H. et al. S-alkylation of cysteine-containing peptides using thianthenium salts as an alkyl source in flow. *Green. Chem.* **26**, 7414–7418 (2024).
48. Ren, J.-X. et al. Site-selective S-gem-difluoroallylation of unprotected peptides with 3,3-difluoroallyl sulfonium salts. *Chem. Sci.* **15**, 10002–10009 (2024).
49. Bao, G. et al. Orthogonal bioconjugation targeting cysteine-containing peptides and proteins using alkyl thianthenium salts. *Nat. Commun.* **15**, 6909 (2024).
50. Haning, H. et al. Imidazo[5,1-f], triazin-4(3H)-ones, a new class of potent PDE 5 inhibitors. *Bioorg. Med. Chem. Lett.* **12**, 865–868 (2002).
51. Jang, I. et al. MS/MS software for screening unknown erectile dysfunction drugs and analogues: artificial neural network classification, peak-count scoring, simple similarity search, and hybrid similarity search algorithms. *Anal. Chem.* **91**, 9119–9128 (2019).

Acknowledgements

This work was supported by the National Natural Science Foundation of China (21972094, 22101185, 22102102, 22372102), National Key Research and Development Program of China (2021YFA1600800), Educational Commission of Guangdong Province (839-0000013131), Shenzhen Science and Technology Program (RCJC20200714114434086, JCYJ20231121175024001), ZDSYS201707271014468; the City University of Hong Kong startup fund (9020003), ITF-RTH-Global STEM Professorship (9446006), MEXT (20H05838, 24H00485, 24K21809) and the Guangdong Basic and Applied Basic Research Foundation (2020A1515010982).

Author contributions

C.S. and W.O. conceived the project. H.H. and W.O. synthesized the materials, explored the substrate scope, and built the SPS-based continuous-flow platform. Y.T., T.C., and J.W. assisted with materials characterization and data analysis. Q.W., W.L., Q.X., and L.Y. advised on organic experiments. W.O. wrote the draft, with the assistance of C.S. and B.L. All authors discussed the results and edited and commented on the manuscript.

Competing interests

The authors declare no competing interests.

Additional information

Supplementary information The online version contains supplementary material available at <https://doi.org/10.1038/s41467-025-65810-z>.

Correspondence and requests for materials should be addressed to Chenliang Su.

Peer review information *Nature Communications* thanks Xinxin Shao, and the other, anonymous, reviewers for their contribution to the peer review of this work. A peer review file is available.

Reprints and permissions information is available at <http://www.nature.com/reprints>

Publisher's note Springer Nature remains neutral with regard to jurisdictional claims in published maps and institutional affiliations.

Open Access This article is licensed under a Creative Commons Attribution-NonCommercial-NoDerivatives 4.0 International License, which permits any non-commercial use, sharing, distribution and reproduction in any medium or format, as long as you give appropriate credit to the original author(s) and the source, provide a link to the Creative Commons licence, and indicate if you modified the licensed material. You do not have permission under this licence to share adapted material derived from this article or parts of it. The images or other third party material in this article are included in the article's Creative Commons licence, unless indicated otherwise in a credit line to the material. If material is not included in the article's Creative Commons licence and your intended use is not permitted by statutory regulation or exceeds the permitted use, you will need to obtain permission directly from the copyright holder. To view a copy of this licence, visit <http://creativecommons.org/licenses/by-nc-nd/4.0/>.

© The Author(s) 2025